

Preliminary Design of System-integrated Heat Exchangers for Passive Molten Salt Fast Reactor

Jihun Im^a, Jae Hyung Park^a, Won Jun Choi^a, *Sung Joong Kim^{a, b}.

^a Department of Nuclear Engineering, Hanyang University, 222 Wangsimni-ro, Seongdong-gu, Seoul 04763, Republic of Korea

^b Institute of Nano Science and Technology, Hanyang University, 222 Wangsimni-ro, Seongdong-gu, Seoul 04763, Republic of Korea

* Corresponding author: sungjkim@hanyang.ac.kr

1. Introduction

Molten salt reactors (MSRs) have emerged as a promising low-carbon energy solution, offering improved efficiency, safety, and waste reduction. However, concerns about proliferation risks in liquid fuel MSR systems persist.

To address these issues, the I-SAFE-MSR Research Center in South Korea has developed the Passive Molten Salt Fast Reactor (PMFR). Notably, the PMFR employs natural circulation in the reactor loop, eliminating the need for mechanical pumps handling high-temperature and radiant fluids [1]. The PMFR features a helical coil heat exchanger, a type commonly used in compact systems with spatial limitations, as seen in SMRs like SMART and NuScale.

The design of the PMFR's heat exchanger is crucial for evaluating the feasibility of the natural circulation concept. Flow rate, directly linked to the reactor's power output, is impacted by the pressure drop in the heat exchanger, significantly influencing natural circulation. Additionally, the heat transfer area plays a pivotal role, as excessive or insufficient area can limit reactor output and power conversion efficiency.

This study aims to assess the feasibility of the PMFR concept through a parametric sensitivity analysis of the heat exchangers. The analysis involves evaluating the performance of the helical coil heat exchanger using one-dimensional modeling with calculation results of the PMFR's natural circulation. Subsequently, a SCO₂ cycle analysis utilizes these results as input values. Finally, the study compares the electrical output of the PMFR based on various heat exchanger design parameters.

2. Modeling of PMFR primary loop

2.1 PMFR loop models

Figure 1 depicts the schematic diagram of the PMFR reactor system. The system is composed of a core, a riser, helical-coil heat exchanger tubes enveloping the riser, and a downcomer. Helium is introduced into the core from the bottom, ascending with the fuel salt, and subsequently undergoing separation. Consequently, the core and riser undergo two-phase flow, while the heat exchangers and downcomers are represented as single-phase flow. The separator is modeled as a basic cylindrical tank with a metallic mesh screen.

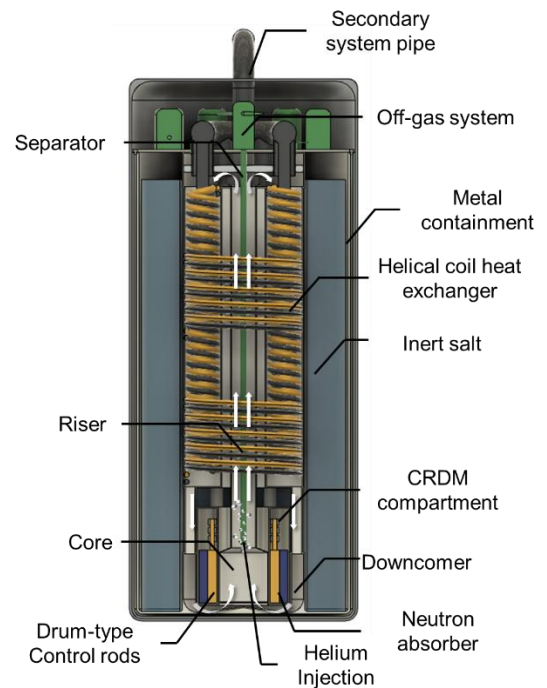


Figure 1 Schematic diagram of PMFR reactor system

The fuel salt chosen for this study was the UCl₃-UCl₄-KCl system, and its thermodynamic properties were obtained from experimental measurements [2]. The properties of helium were evaluated using the National Institute of Standards and Technology (NIST) database program. The temperature of helium was assumed to be the same as the fuel salt, but heat transfer between the two fluids was neglected.

The heat generation of the core was analyzed using a homogeneous cylindrical reactor model, while the decay heat of the fuel was neglected to simplify the analysis.

$$Q = \dot{m} c_p \Delta T = \sum_i \frac{\pi Q}{2H_{core}} * \sin\left(\frac{\pi}{H_{core}} z(i)\right) dz \quad (1)$$

2.2 Hydraulic models for PMFR loop

In this preliminary analysis, the impact of decay heat was disregarded. Consequently, the mass flow rate of the fuel salt was determined based on the energy balance equation.

The salt circulation cycle within this system can be divided into two trajectories: an ascending path originating from the base of the core and extending to the upper surface of the separator, and a descending route back to the core through the heat exchangers and downcomers. For the analysis, both paths were discretized into 250 segments in the z -direction.

Under steady-state conditions, the elevation of the salt remained constant. Consequently, the velocity at node 1 was assumed to be zero. Additionally, the pressure at nodes 1 and 250 in each trajectory was considered identical, enabling the formulation of pressure balance equations for both paths. In this context, the index i represents the node number, ranging from 1 to 250.

For upward path,

$$P_n + \sum_i^n (\rho g \Delta z) + \sum_i^n P_{loss} = P_1 + \left(\frac{1}{2} \rho_i v_i^2 \right)_{t,p} \quad (2)$$

For downward path,

$$P_n + \sum_i^n (\rho_i g \Delta z) = P_1 + \left(\frac{1}{2} \rho_i v_i^2 \right) + \sum_i^n P_{loss} \quad (3)$$

Subscripts t,p means the two-phase flow state.

The core and riser were modeled as the cylindrical pipe, and the two-phase flow friction loss was evaluated by applying Lockhart and Martinelli [3] approach.

$$\Delta P_{t,p} = \Phi^2 \left(f \frac{L}{D} \frac{1}{2} \rho v^2 \right)_{f,superficial} \quad (4)$$

$$\Phi^2 = 1 + \frac{C}{X_{tt}} + \frac{1}{X_{tt}^2} \quad (5)$$

$$X_{tt} = \left(\frac{1-x}{x} \right)^{0.9} \left(\frac{\rho_{He}}{\rho_f} \right)^{0.5} \left(\frac{\mu_f}{\mu_{He}} \right)^{0.1} \quad (6)$$

X_{tt} and Φ are Lockhart and Martinelli parameters and the two-phase friction multiplier.

The reduction pressure loss of the flow channel between the core and the riser was evaluated by the following correlation:

$$\Delta P_{reduction} = \left(1 - \frac{D_{riser}^2}{D_{core}^2} \right) \left(\frac{1}{2} \rho v^2 \right)_{t,p} \quad (7)$$

2.3 PMFR heat exchanger models

The helical coil heat exchanger consists of a passage for secondary side tubes, a central column that functions as a support for the tube bank, a helical coil tube bank, and a shell that encloses the entire heat exchanger. The arrangement of the tube bank can be either in-lined or staggered.

The PMFR molten salt fuel was designed to flow from top to bottom on the shell side of the mentioned helical coil heat exchanger. This is to reduce the effect of pressure drop in the PMFR loop driven by natural circulation. The secondary side salt was preliminarily designed to flow from the bottom to the top along the

tube. This crossflow configuration is advantageous in maintaining a constant temperature difference in heat transfer between the two fluids and maximizing the amount of heat transfer.

The molten salt on the tube side of the heat exchanger adopted the NaBF₄-NaF system adopted by MSBR [4]. The thermal salt has excellent thermal properties and low cost. For this preliminary analysis, the adopted system parameters are summarized and listed in **Table 1**.

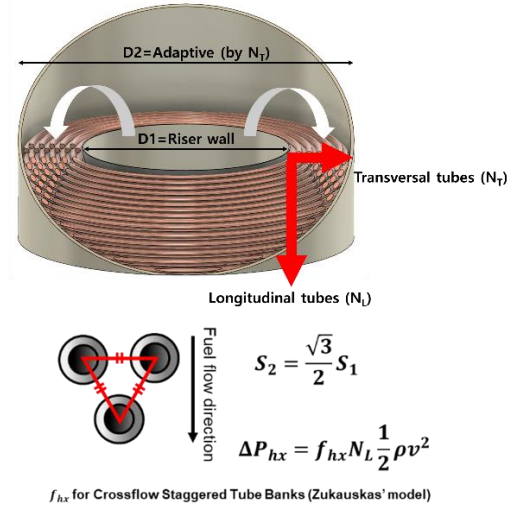


Figure 2 Helical coil heat exchanger model [8]

Table 1. Design parameters of the PMFR system.

Parameters	Values
Reactor	
Helium injection rate	0.1 kg/sec
Core diameters	2 m
Core length	2 m
Riser diameters	1 m
Riser length	13 m
Core inlet-outlet temp.	600°C–750°C
Fuel salt properties	
	UCl ₃ – UCl ₄ – KCl
Heat capacity	98.90 J/mol·K
Viscosity [2]	3.5 cP – 2.0 cP
Density [2]	3142.5 kg/m ³ – 3003.3 kg/m ³
Thermal conductivity	Assumed (0.5 W/mK)
Thermal salt properties [4]	
	NaBF ₄ -NaF
Salt composition	92 % - 8 %
Heat capacity	1750 J/kgK
Viscosity	0.09 cP
Density	1507 kg/m ³
Thermal conductivity	0.4 W/mK

The heat exchanger model was based on the imperial correlations using the research results of Zukauskas [5] for the shell side and Schmidt [6] for the tube side. The

mass flow rate of the thermal salt on the secondary side was calculated based on the mass flow rate of the primary fuel salt, which is set to have the same heat capacity as the primary PMFR side. The iterative calculations were used to determine the secondary heat exchanger inlet temperature of thermal salt, which was adjusted to achieve the desired primary heat exchanger outlet temperature of 600°C.

2.4 SCO_2 recompression cycle models

The SCO_2 recompression cycle represents an enhancement over the basic recuperated SCO_2 cycle, incorporating an additional compression stage. In a straightforward recuperated cycle, the SCO_2 undergoes cooling through a recuperator and a precooler after passing through the turbine before undergoing compression once again. However, a challenge arises due to a pinch-point issue caused by the varying specific heat based on SCO_2 pressure within the recuperator. The recompression cycle addresses this specific heat disparity by dividing the SCO_2 mass flow rate. It compresses a portion of the less cooled SCO_2 , thereby reducing the mass flow rate of the colder segment with a relatively high specific heat value. The arrangement of the recompression cycle is illustrated in **Figure 4**.

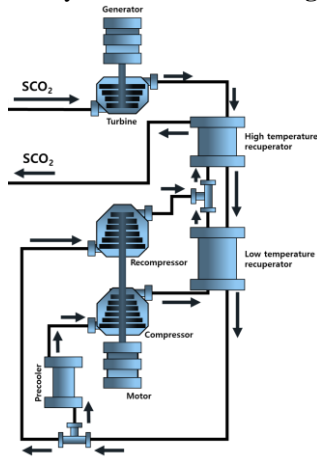


Figure 3 schematic of SCO_2 recompression cycle

By utilizing the temperature range of the secondary system thermal salt derived from the PMFR loop and heat exchanger model, the input parameters for the SCO_2 cycle analysis code, including the turbine inlet temperature and SCO_2 flow rate, were established. The turbine inlet temperature was designated as 10 °C lower than the maximum temperature of the secondary system. The SCO_2 flow rate was computed based on the heat transferred from the intermediate heat exchanger. The mass split ratio and pressure ratio of the turbomachinery underwent optimization, considering the maximum pressure and temperature. The cycle efficiency was then calculated using the optimized mass split ratio and pressure ratio, and the electrical output was determined by multiplying the PMFR fission heat by the efficiency.

Table 2. Parameters of the SCO_2 recompression cycle.

Parameters	Values
Isentropic efficiency of compressors	0.85
Isentropic efficiency of turbine	0.92
Minimum pinch point temperature differences of the heat exchangers	10 °C
Compressor inlet temperature	32 °C
Turbine inlet pressure	25 MPa

2.5 Test matrix

This study designates the transversal tubes and longitudinal tubes of this heat exchanger as the main sensitivity parameters. These parameters directly influence the heat transfer area with maintaining the specified tube pitch. The transversal tubes are equivalent to the parallel channels in the heat exchanger, and an increase in their number expands the flow path of the heat exchanger. To prevent potential drawbacks from an excessive number of transversal tubes in terms of the overall system volume, a maximum limit of 22 rows was imposed.

The longitudinal tubes, on the other hand, increase the length of the heat exchanger but are constrained by the length of the riser. In this study, we set a maximum of 290 rows, corresponding to a length of 12.55 meters. This approach aims to optimize the heat exchanger design by balancing the effects of transversal and longitudinal tubes while considering practical constraints.

Table 3. Parameters of the helical coiled heat exchanger

Heat exchangers	Helical coil
Tubes outer diameter	25 mm
Tubes inner diameter	23 mm
Transversal P/D	2.0 (P=50 mm)
Longitudinal P/D	$\sqrt{3}$
Numbers of modules	6 ea
Transversal tube-rows	13 – 22
Longitudinal tube-rows	100 – 290
Tube conductivity	45 W/mK

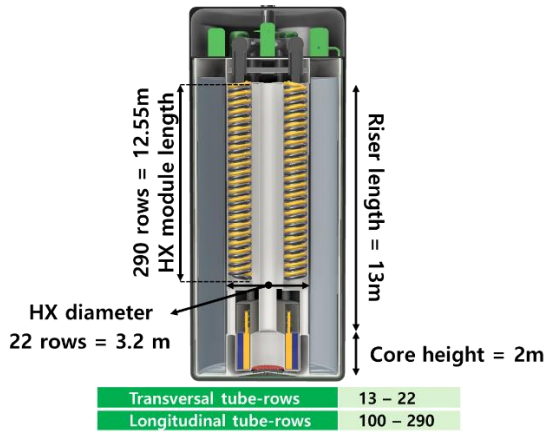


Figure 4 Test matrix of the heat exchanger parameters

3. Results & Discussion

Ensuring that the circulation power of the nuclear fuel salt, aligned with the thermal power of 300 MWt in the PMFR, can effectively overcome the pressure drop in the heat exchanger is crucial. To evaluate this, the pressure margin was calculated, and the determination is based on the following equation.

$$\int \rho_{down(z)} g z dz - \int \rho_{up(z)} g z dz = (\sum P_{loss})_{known} + P_{margin} \quad (8)$$

The left side represents the natural circulation driving force, and the right side denotes the pressure drop component within the system. The difference between these two is defined as the pressure margin.

Figure 5 illustrates the analysis findings of the pressure margin concerning the provided test matrix. With an increase in the number of transversal tubes, the expanded flow path and reduced velocity in each channel contribute to maintaining the pressure margin. Conversely, an escalation in longitudinal tubes results in an overall rise in pressure drop within the heat exchanger, causing a decline in the pressure margin. The slope of this reduction becomes more noticeable when the number of transversal tubes is low.

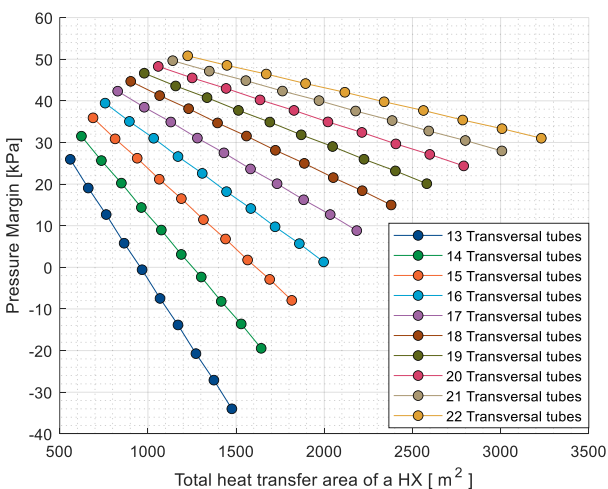


Figure 5 Pressure margin for the heat exchanger parameters

Figure 6 illustrates the relationship between the total heat transfer area of the heat exchanger (HX) and the cycle efficiency (%) through a scatter plot. Only data with a positive pressure margin were utilized.

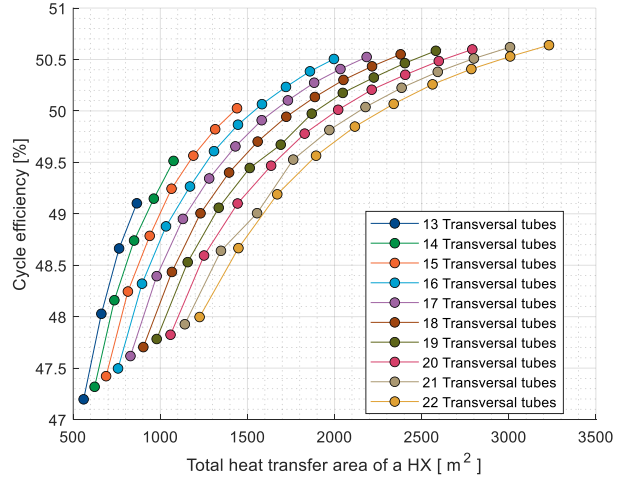


Figure 6 Energy conversion system efficiency for the heat exchanger parameters

As the longitudinal tubes increases, there is a corresponding increase in cycle efficiency, consistently observed regardless of the number of transversal tubes. The series of points form an upward trendline, indicating that as the total heat transfer area increases, the cycle efficiency also increases.

Comparing the cases with 16 transversal tubes and 22 transversal tubes, it is evident that despite a 60% increase in system size, the cycle efficiency shows only a marginal difference, with values of 50.5% and 50.64%, respectively. This finding suggests that, from an overall cost perspective in the PMFR system, the increase in system size may pose a drawback with inferior improvement in cycle efficiency.

Based on this analysis, the feasibility of the PMFR heat exchanger design could be assessed in terms of power conversion performance and ensuring natural circulation flow. The pressure margin was highly dependent on the number of transversal tubes. A minimum of 16 transversal tubes would be required to achieve a 12.5m level heat exchanger, and 15 or fewer would require a shorter heat exchanger area to ensure natural circulation flow.

In the heat exchanger parameter range that satisfies the above conditions for ensuring the natural circulation flow rate, the power conversion efficiency was 47.2% to 50.64%. This is a superior power generation efficiency compared to the current light water reactor systems. Therefore, the natural circulation operation of the PMFR is considered reasonable with appropriate heat exchanger selection.

4. Conclusion

In conclusion, this study conducted a comprehensive assessment of the PMFR concept by performing a parametric sensitivity analysis of the heat exchangers.

The analysis findings, as illustrated in Figures 5 and 6, provide valuable insights. The results demonstrate a positive relationship between the total heat transfer area of the heat exchanger and cycle efficiency, consistently observed with an increase in longitudinal tubes, regardless of the number of transversal tubes. This suggests that an expanded total heat transfer area contributes to enhanced cycle efficiency.

However, comparing cases among transversal tubes, despite sharply increase in system size, the cycle efficiency shows only a marginal difference. These findings highlight that the increase in system size may pose a drawback from an overall cost perspective in the PMFR system, as it results in only a minor improvement in cycle efficiency.

In summary, the study provides valuable insights into the critical factors influencing the performance of the PMFR concept and offers considerations for optimizing its design.

steam generator in high temperature gas reactors with genetic algorithm and response surface method. *Energy*, 259.

Acknowledgments

This research was supported by the National Research Foundation of Korea (NRF) and funded by the ministry of Science, ICT, and Future Planning, Republic of Korea, grant numbers (NRF-2021M2D2A2076382) and (RS-2023-00261295)

REFERENCES

- [1] J. Lim, D. Shin, T. Kim, J. H. Park, J. Lee, Y. S. Cho, Y. Kim, S. Kim, S. J. Kim, Preliminary Analysis of the Effect of the Gas Injection on Natural Circulation for Molten Salt Reactor Type Small Modular Reactor System Operated without a Pump, *Transactions of the Korean Nuclear Society Virtual Autumn Meeting October 21-22 (2021)*
- [2] S. Katyshev, Yu Chervinskii, V. Desyatnik. Density and viscosity of fused mixtures of uranium chlorides and potassium chloride. *Atomic Energy*, (1982).
- [3] R.W. Lockhart, R.W. Martinelli, Proposed correlation of data for isothermal twophase, two-component flow in pipes. *Chem. Eng. Process.* 45, 39–48, (1949).
- [4] Sabharwall, Piyush, et al. Process heat exchanger options for fluoride salt high temperature reactor. No. INL/EXT-11-21584. Idaho National Lab.(INL), Idaho Falls, ID (United States), (2011).
- [5] Zukauskas, A., and Romanas Ulinskas. "Heat transfer in tube banks in crossflow." (1988).
- [6] Schmidt, Eckehard F. "Wärmeübergang und druckverlust in roherschlangen." *Chemie Ingenieur Technik* 39.13 (1967).
- [7] J.H. Lim, J.G Jeon, J.H Park, D.Y. Shin S.J. Kim, Thermodynamic study of SCO₂ Recompression Brayton Cycle with Intercooling and Reheating for Light Water Reactor, *Transactions of the Korean Nuclear Society Autumn Meeting*, 2020
- [8] Sun, J., Zhang, R., Wang, M., Zhang, J., Qiu, S., Tian, W., & Su, G. (2022). Multi-objective optimization of helical coil